

Neutron scattering study of a membrane phase miscibility gap: Coexistence of L_3 “sponge” and L_α Lamellar phases

W A Hamilton^{1,†} and L Porcar²

¹Bragg Institute, Australian Nuclear Science and Technology Organisation, Lucas Heights, Australia

²Large Scale Structures Group, Institut Laue-Langevin, Grenoble, France

Email: Hamilton.WA@gmail.com

Abstract. We report on a small angle neutron scattering (SANS) study of a temperature driven first order phase transition in a 25wt% solution of the surfactant AOT (Sodium Di-2-ethylhexyl Sulfosuccinate) in 1.5wt% heavy brine between an isotropic L_3 “sponge” state at 27°C and a stacked lamellar L_α monophasic 55°C. The prominent scattering features of these phases are correlation peaks due to the mean passage size of the L_3 sponge and the L_α stacking separation. This ratio of the monophasic peak positions $Q_\alpha/Q_3 \approx 1.3$, is consistent with previous observations in this and similar systems. In the present study we tracked this system through the intermediate $L_3 + L_\alpha$ biphasic miscibility gap. There the initial appearance of the L_α peak at 33.25°C was at a scattering vector some 23% higher than the final high temperature monophasic value. During coexistence both L_3 and L_α phase peak positions decreased linearly with increasing temperature maintaining a roughly constant ratio $Q_\alpha/Q_3 \sim 1.6-1.7$. Two phase fits to the scattering data and application of scaling law predictions allow us to obtain local L_3 phase volume fractions in the biphasic region and make preliminary determinations of the structural accommodations necessitated by phase coexistence in this system’s miscibility gap.

1. AOT membrane phases and scaling laws

AOT (Sodium Di-2-ethylhexyl Sulfosuccinate) is a double tailed anionic surfactant which displays a variety of self-assembled mesophases in aqueous solution[1]. Over a range of concentrations and temperatures in brine solution AOT molecules self-assemble into bilayer membranes with the surfactants headgroup on the exterior shielding the hydrophobic tails from the solvent. Among the mesophases that may be formed by arrangement of these membranes are the familiar anisotropic L_α lamellar phase in which membranes are ordered as separated stacks and the isotropic L_3 bicontinuous “sponge” phase in which the membranes are connected by random passages to form an isotropic network that spans the solution[2]. These topological differences result in distinct material properties: L_α phases are relatively viscous and optically birefringent, while L_3 phases are free flowing and optically inactive. In small angle neutron and x-ray scattering (SANS and SAXS) measurements the L_α phase gives rise to sharp quasi-Bragg scattering peak due to the stacking separation, while for L_3 a broader correlation peak characteristic of the mean passage size is observed. These morphologies are

[†] To whom any correspondence should be addressed

often found adjacent to one another in the phase diagram, with the phase behavior being driven by the intrinsic curvature of the bilayer, which may vary with temperature (as in the current case), pressure, membrane or solvent composition.

Over a broad range of dilution these phases follow a “sheet” scaling equation where the membrane volume fraction ϕ is proportional to the membrane thickness δ divided by the characteristic length scale of the structure d , to a constant of proportionality C depending on their morphology. For rigid flat membranes stacked with period d we can see from Figure 1 that $C \equiv 1$. Surfactant bilayers are not totally rigid, so ripples diminish the projected area normal to stacking and membranes are more distant for a given ϕ so C is a little greater than unity. Similarly the L_3 phase may be considered as a distorted version of the Shwartz “P” regular cubic structure which has a constant negative Gaussian sheet curvature. For this structure with d as the passage width a value $C \approx 1.486$ has been estimated numerically[3]. For sponge phases the width of their scattering correlation peak indicates a greater variation of local curvature and passage size so we may expect C to be somewhat greater than 1.5.

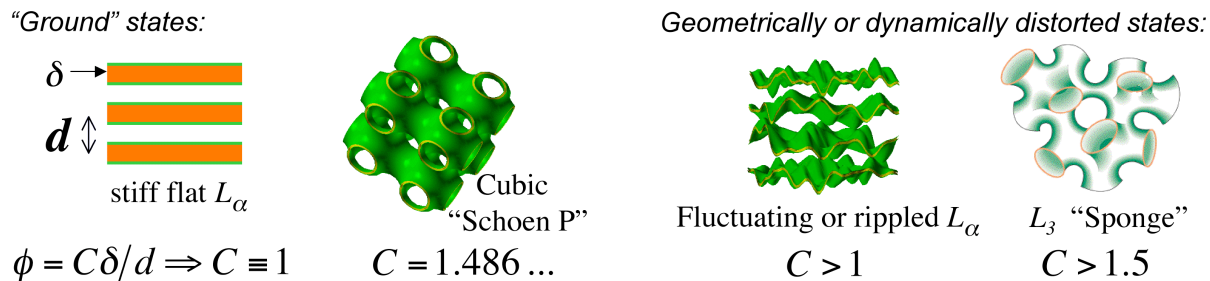


Figure 1. Membrane morphology and sheet equation coefficient of proportionality.

2. Scattering measurements over the L_3 to L_α phase transition miscibility gap

In this paper we briefly report on a small angle neutron scattering (SANS) study of 25wt% solution of the surfactant AOT in 1.5wt% heavy brine between 27°C and 55°C over which range decreasing intrinsic curvature of the surfactant bilayer drives the system from an initial L_3 state to a final L_α state. In an intermediate miscibility gap region microphase regions of the L_α phase nucleate within the L_3 phase and we find coexistence of the two morphologies. Our measurements were taken on the SAND time-of-flight (TOF) SANS instrument at the Intense Pulsed Neutron Source (IPNS) at Argonne National Laboratory (ANL). SANS measurements of 30m duration were taken on a 1mm thick sample in a quartz cell in 4°C steps (controlled to about 0.1°C), and in finer steps over the range ~31–34°C where the onset of the transition was expected from observed optical birefringence.

Figure 2(a) shows SANS over the full scattering vector Q range measured (to about 1.0 \AA^{-1}) for the L_3 and L_α monophases at 27°C and 55°C. At 27°C the broad L_3 correlation peak at $Q=0.062 \text{ \AA}^{-1}$ corresponds to a mean passage size of 101 Å. At 55°C the narrower quasi-Bragg L_α peak at $Q=0.079 \text{ \AA}^{-1}$ indicates a membrane stacking separation of 79 Å. This ratio of monophase peak positions and inversely correlation lengths $Q_\alpha/Q_3 = d_3/d_\alpha = 1.27$ is consistent with previous observations in this and similar systems (for instance [4] and [5]). Figure 2(b) shows the evolution of the scattering in the correlation peak region. As the temperature was increased we observed no significant change until the biphasic boundary is crossed, signalled in our data by the first detectable appearance of an L_α peak at 33.25°C at $Q=0.103 \text{ \AA}^{-1}$ some 23% higher than the final monophase value at 55°C and indicating an initial L_α separation of only 61 Å. Both peaks then move to lower Q , with the L_3 peak weakening, to become undetectable in our 55°C data, as the L_α peak becomes stronger.

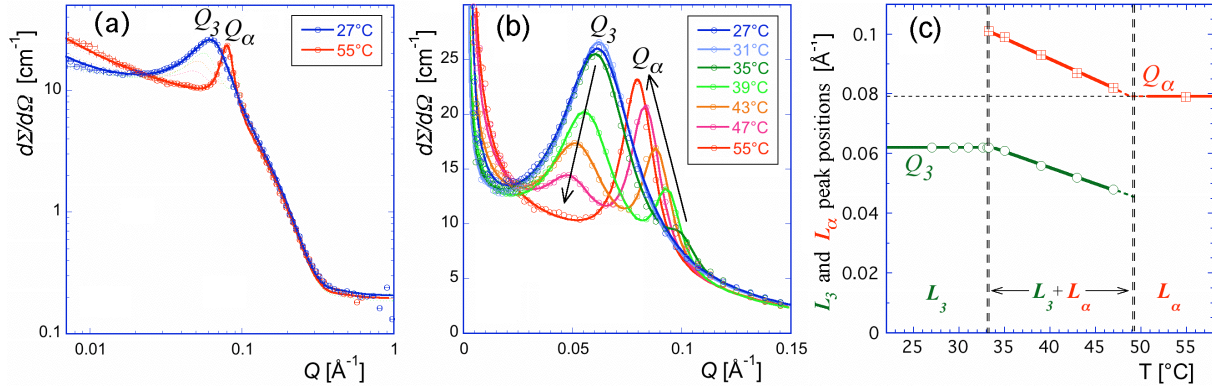


Figure 2. Data and fits for 25wt% AOT in 1.5wt% heavy brine. (a) SANS for 27°C L_3 and 55°C L_α monophases. (b) SANS as transition proceeds. (c) Q_3 and Q_α peak position versus temperature.

3. Scattering data fitting

Fits to our SANS measurements shown were obtained using the scattering function:

$$\frac{d\Sigma}{d\Omega}[Q] = NV^2(\Delta\rho)^2 P[Q] S[Q] + I_{bg} \quad (1)$$

$$\equiv \left(\frac{\pi \phi \sigma^2 (\Delta\rho)^2}{(t_o + t_h)} \right) \left(\frac{4(1 - \cos[Qt_o] \exp[-Q^2 \delta_o^2 / 2])}{Q^2 (\sigma^2 + 2 \exp(-Q^2 \sigma^2 / 6))} \right) \left(1 + \frac{A_3}{Q} + \frac{B_3}{1 + (Q - Q_3)^2 \xi_3^2} + \frac{B_\alpha}{1 + (Q - Q_\alpha)^2 \xi_\alpha^2} \right) + I_{bg}$$

The first two terms in braces of the second line capture in an analytic form[6] the number density N , scattering power (as the square of volume multiplied by the neutron contrast) and form factor (P) of randomly oriented discoids of membrane of rms radius σ , of contrast (tail) thickness t_o with and bilayer surface (headgroup) thickness t_h with a rms variation in thickness δ_o , which are arranged in mesophases described by the third term, a structure factor (S). This coherent scattering sits on an incoherent background I_{bg} (0.19 cm^{-1} from our fits). For measurements on a single sample the first braced term is a constant scaling parameter. From our fits we found $t_o = 15.5 \pm 0.5 \text{ \AA}$ with δ_o , about one quarter of this thickness $\sim 3.8 \text{ \AA}$, typical of surfactant membranes[7]. This second form factor term dominates at higher Q , where we observe a shoulder at $Q \sim 0.18 \text{ \AA}^{-1}$ as the scattering changes from $\sim Q^2$ behavior characteristic of membrane scattering to the $\sim Q^4$ dependence of surface scattering (see Figure 2(a)). This feature and a slight shift to lower Q with increasing temperature was reproduced by a gradual increase in the form factor disc radius σ from 11.0 \AA at 27°C to 12.7 \AA at 55°C, as we might expect going from the highly curved L_3 to the flatter L_α phase.

In our structure factor[8] the L_3 and L_α peaks are modelled as Lorentzians at Q_3 and Q_α with correlation lengths ξ_3 and ξ_α . The A_3/Q is term is intended to fit long range “in-out” scattering attributed the L_3 membrane’s division of the solvent volume[9]. This term was adequate to fit the obvious increase in low Q scattering as the transition proceeds adequately, due perhaps to L_α phase domain formation, over this Q range. Our fits to this series were all averaged over resolution of the reduced TOF SANS data (see horizontal error bars in Figure 2(a)), which maintains a constant ratio of variance to Q (i.e. $\sigma_Q^2/Q \sim 0.0003 \text{ \AA}^{-1}$) but does not significantly broaden any scattering features[10]. Some parameters obtained from our data series fits are presented in Table 1.

4. Preliminary results and interpretation

Figure 3(a) graphs the variation in L_3 and L_α peak positions Q_3 and Q_α peak positions showing their linear variation with temperature over the miscibility gap. Extrapolating this variation of Q_α to its monophase limit at 55°C we may determine that the upper boundary of $L_3 + L_\alpha$ coexistence occurs at 49°C. In the $L_3 + L_\alpha$ region the ratio Q_α/Q_3 gradually increases from 1.61 to 1.71 between 33.25°C and

the last measurement in this region at 47°C. We note that this is close to the “ground state” value for Q_α/Q_3 we might infer from Section 1. Assuming the scaling relation holds for L_3 over the biphasic region, which seems reasonable as the normalized correlation width of the L_3 structure factor peak is constant at $(\xi_3 Q_3)^{-1} \sim 0.30$ over it, we may extract the local volume fraction within the L_3 phase domains, $\phi_3[T]$. This will simply be proportional to $1/d_3[T] \propto Q_3[T]$. We present $\phi_3[T]$ in Table 1 - normalized to the L_3 monophasic value at 27°C. In principle this value can be used to determine the “tie-line” boundaries of L_3+L_α coexistence versus temperature in the system phase diagram over a range near the current volume fraction. Another value which may be extracted is the effective “matching angle” $\theta = \sin^{-1}(d_\alpha/d_3)$ between the mesophase bilayer periodicities at their microphase boundaries. We see that this angle is $\sim 37^\circ$ over the biphasic region in our system. This is rather lower than the $\sim 50-60^\circ$ deduced by Quillet *et al.*[4] for L_3+L_α coexistence in the CetylPyridinium Chloride/Hexanol membrane system. It is possible that this difference and the behavior of the biphasic ratio of Q_α/Q_3 may be due to the greater stiffness of and local curvature constraints on bilayers formed by AOT as a double tailed surfactant[11].

Table 1. Structure factor fitting parameters and derived local sponge volume fraction and phase contact angle values obtained from our data for the L_3 to L_α phase transition over the measured range. The Lorentzian widths of correlation peaks ξ_3^{-1} and ξ_α^{-1} have been normalized to peak position values.

T [°C]	A_3 [cm ⁻¹]	B_3 [cm ⁻¹]	Q_3 [Å ⁻¹]	$(\xi_3 Q_3)^{-1}$	$\phi_3[T]/\phi_3[27^\circ\text{C}]$ $\approx Q_3[T]/Q_3[27^\circ\text{C}]$	B_α [cm ⁻¹]	Q_α [Å ⁻¹]	$(\xi_\alpha Q_\alpha)^{-1}$	Q_α/Q_3 $= d_3/d_\alpha$	θ [°] $= \sin^{-1}(d_\alpha/d_3)$
27	0.008	3.5	0.062	0.34	1.00	0.0	-	-	-	-
31	0.004	3.5	0.064	0.29	1.02	0.0	-	-	-	-
33.25	0.004	3.5	0.064	0.28	1.02	0.2	0.103	0.05	1.61	38.4
35	0.005	3.2	0.063	0.29	1.00	0.7	0.100	0.057	1.61	38.4
39	0.006	2.1	0.057	0.28	0.92	1.9	0.094	0.068	1.65	37.3
43	0.009	1.4	0.053	0.30	0.85	2.6	0.089	0.079	1.68	36.5
47	0.014	0.8	0.049	0.3	0.80	3.3	0.084	0.089	1.71	35.7
55	0.016	0.0	-	-	-	3.7	0.08	0.099	-	-

Acknowledgements

This research sponsored by the Office of Basic Energy Sciences, U.S. Department of Energy under contracts DE-AC05-00OR22725 with Oak Ridge National Laboratory(ORNL) and W-31-109-ENG-38 with ANL. The help given of IPNS and SAND personnel was greatly appreciated. Fits to the data are from the MIRROR program developed by J B Hayter and W A Hamilton (1992–2005).

References

- [1] O Ghosh and C A Miller 1987 *J. Phys. Chem.* **91** 4528
- [2] G Porte 1999 From giant micelles to fluid membranes *Soft Matter Physics* ed M Daoud and C E Williams (Berlin, Springer-Verlag) chapter 5 p 155
- [3] I S Barnes, S T Hyde, B W Ninham, P J Derian, M Drifford, G G Warr and T Zemb 1988 *Prog. Colloid Polym. Sci.* **1** 358
- [4] C Quillet, C Blanc and M Kléman 1996 *Phys. Rev. Lett.* **77** 522
- [5] W A Hamilton, L Porcar, P D Butler and G G Warr 2002 *J. Chem. Phys.* **116** 8533
- [6] L Porcar, W A Hamilton, P D Butler and G G Warr 2003 *Langmuir* **19** 10779
- [7] F. Nallet, R. Laversanne, and D. Roux, *J. Phys. II* **3**, 487 ~1993
- [8] Modified from: N Lei, C R Safinya, D Roux, and K S Liang 1997 *Phys. Rev. E* **56** 608
- [9] D Roux and C Coulon 1992 *J. Phys. Chem.* **96** 4174
- [10] R P Hjelm 1987 *J. Appl. Cryst.* **20** 273
SAND web page <http://www.pns.anl/instruments/sand/> (download 29 April 2003)
- [11] O D Lavrentovich, C Quillet and M Kléman 1997 *J. Chem. Phys.* **101** 420